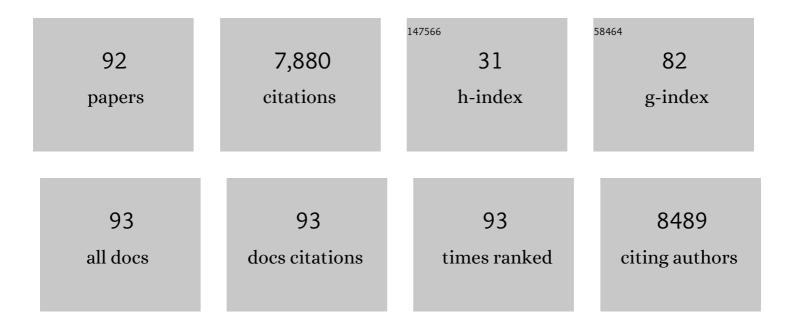
List of Publications by Year in descending order

Source: https://exaly.com/author-pdf/2359118/publications.pdf Version: 2024-02-01



#	Article	IF	CITATIONS
1	Degradable mesoporous semimetal antimony nanospheres for near-infrared II multimodal theranostics. Nature Communications, 2022, 13, 539.	5.8	17
2	Optimal weak measurement in the photonic spin Hall effect for arbitrary linear polarization incidence. Optics Express, 2022, 30, 4096.	1.7	10
3	Chiral Ligand-Induced Structural Transformation of Low-Dimensional Hybrid Perovskite for Circularly Polarized Photodetection. Chemistry of Materials, 2022, 34, 2955-2962.	3.2	24
4	Nonlinear-dependent h-shaped pulse generation in a Raman fiber laser. Optics and Laser Technology, 2022, 151, 108055.	2.2	3
5	Short-pulsed Raman fiber laser and its dynamics. Science China: Physics, Mechanics and Astronomy, 2021, 64, 1.	2.0	30
6	Correlation between geometric parametric instability sidebands in graded-index multimode fibers. Chaos, 2021, 31, 013109.	1.0	2
7	Weak measurements of the waist of an arbitrarily polarized beam via in-plane spin splitting. Optics Express, 2021, 29, 8777.	1.7	10
8	Real-time observation of Q-switched mode-locking in a tin selenide modulated ultrafast fiber laser. Applied Physics Express, 2021, 14, 042009.	1.1	5
9	Antimony Nanopolyhedrons with Tunable Localized Surface Plasmon Resonances for Highly Effective Photoacousticâ€Imagingâ€Guided Synergistic Photothermal/Immunotherapy. Advanced Materials, 2021, 33, e2100039.	11.1	32
10	Gas sensing near exceptional points. Journal Physics D: Applied Physics, 2021, 54, 254001.	1.3	11
11	Enhanced spin Hall effect due to the redshift gaps of photonic hypercrystals. Optics Express, 2021, 29, 12160.	1.7	24
12	Recognizing fractional orbital angular momentum using feed forward neural network. Results in Physics, 2021, 28, 104619.	2.0	18
13	3.46Âμm Q-switched Er3+:ZBLAN fiber laser based on a semiconductor saturable absorber mirror. Optics and Laser Technology, 2021, 141, 107131.	2.2	10
14	Enhanced photonic spin Hall effect via singularity induced by destructive interference. Optics Letters, 2021, 46, 4883.	1.7	7
15	High energy switchable pulsed High-order Mode beams in a mode-locking Raman all-fiber laser with high efficiency. Optics Express, 2021, 29, 40538.	1.7	5
16	Dye-Sensitized Lanthanide-Doped Upconversion Nanoparticles for Water Detection in Organic Solvents. ACS Applied Nano Materials, 2021, 4, 14069-14076.	2.4	7
17	Ultra-compact, low-loss terahertz waveguide based on graphene plasmonic technology. 2D Materials, 2020, 7, 015016.	2.0	24
18	Short-cavity random distributed feedback fiber laser with ultra-low threshold. Applied Physics Express, 2020, 13, 012008.	1.1	1

#	Article	IF	CITATIONS
19	Actively manipulating asymmetric photonic spin Hall effect with graphene. Carbon, 2020, 166, 396-404.	5.4	32
20	H-shaped pulse generation with tunable leading edge from a Tm-doped mode-locked fiber laser. Applied Physics Express, 2020, 13, 012011.	1.1	9
21	Virusâ€Inspired Deformable Mesoporous Nanocomposites for High Efficiency Drug Delivery. Small, 2020, 16, 1906028.	5.2	10
22	Low-threshold stimulated emission in perovskite quantum dots: single-exciton optical gain induced by surface plasmon polaritons at room temperature. Journal of Materials Chemistry C, 2020, 8, 5847-5855.	2.7	8
23	Is eye-level greening associated with the use of dockless shared bicycles?. Urban Forestry and Urban Greening, 2020, 51, 126690.	2.3	21
24	Sub-hundred nanosecond pulse generation from a black phosphorus Q-switched Er-doped fiber laser. Optics Express, 2020, 28, 4708.	1.7	23
25	Controllable nonlinear optical properties of different-sized iron phosphorus trichalcogenide (FePS3) nanosheets. Nanophotonics, 2020, 9, 4555-4564.	2.9	9
26	Passively Q-switched Er3+-doped ZBLAN fiber laser at ~3.5 $\hat{l}^1\!\!/4m$ based on a semiconductor saturable absorber mirror. , 2020, , .		0
27	Two-dimensional tin diselenide nanosheets pretreated with an alkaloid for near- and mid-infrared ultrafast photonics. Photonics Research, 2020, 8, 1687.	3.4	10
28	Spatio-temporal control of dispersive waves trapping by solitons in graded-index multimode fibers. Applied Physics Express, 2020, 13, 112003.	1.1	0
29	Ultra-high order harmonic mode-locking of a Raman fiber laser. Applied Physics Express, 2019, 12, 092002.	1.1	5
30	Comprehensive study on the concept of spectral-domain reflection and refraction. Applied Physics Express, 2019, 12, 102013.	1.1	0
31	Influence of the Organic Chain on the Optical Properties of Two-Dimensional Organic–Inorganic Hybrid Lead Iodide Perovskites. ACS Applied Electronic Materials, 2019, 1, 2253-2259.	2.0	13
32	Orbital angular momentum modes identification of optical vortices using binaural circular aperture. Journal of Optics (United Kingdom), 2019, 21, 065603.	1.0	8
33	Ultra-high light confinement and ultra-long propagation distance design for integratable optical chips based on plasmonic technology. Nanoscale, 2019, 11, 4601-4613.	2.8	32
34	Graded-index breathing solitons from Airy pulses in multimode fibers. Optics Express, 2019, 27, 483.	1.7	11
35	Emission of multiple resonant radiations by spatiotemporal oscillation of multimode dark pulses. Optics Express, 2019, 27, 36022.	1.7	5
36	~3.5 μm self-Q-switched Er3+:ZBLAN fiber laser stabilized by an ASE seeded pump source. , 2019, , .		1

#	Article	IF	CITATIONS
37	Tunable in-plane and transverse spin angular shifts in layered dielectric structure. Optics Express, 2019, 27, 32722.	1.7	9
38	Black phosphorus: broadband nonlinear optical absorption and application. Laser Physics Letters, 2018, 15, 025301.	0.6	27
39	All-inorganic CsPbBr ₃ perovskite quantum dots embedded in dual-mesoporous silica with moisture resistance for two-photon-pumped plasmonic nanoLasers. Nanoscale, 2018, 10, 6704-6711.	2.8	74
40	Thermotunable Terahertz Negative-Index Metamaterials with Dielectric Spheres Embedded in Semiconductor Host. Advances in Condensed Matter Physics, 2018, 2018, 1-6.	0.4	1
41	Switchable dual-wavelength Q-switched fiber laser using multilayer black phosphorus as a saturable absorber. Photonics Research, 2018, 6, 198.	3.4	70
42	A Simple Line Clustering Method for Spatial Analysis with Origin-Destination Data and Its Application to Bike-Sharing Movement Data. ISPRS International Journal of Geo-Information, 2018, 7, 203.	1.4	17
43	Optical event horizon-based complete transformation and control of dark solitons. Optics Letters, 2018, 43, 5327.	1.7	5
44	Coherent Separation Detection for Orbital Angular Momentum Multiplexing in Free-Space Optical Communications. IEEE Photonics Journal, 2017, 9, 1-11.	1.0	10
45	Identification of genetically modified cotton seeds by terahertz spectroscopy with MPGA-SVM. Optik, 2017, 142, 576-582.	1.4	14
46	Switchable phase and polarization singular beams generation using dielectric metasurfaces. Scientific Reports, 2017, 7, 6814.	1.6	31
47	Two-Dimensional Materials Based Optoelectronics. Advances in Condensed Matter Physics, 2017, 2017, 1-2.	0.4	1
48	Analysis of Attraction Features of Tourism Destinations in a Mega-City Based on Check-in Data Mining—A Case Study of Shenzhen, China. ISPRS International Journal of Geo-Information, 2016, 5, 210.	1.4	35
49	Van der Waals stacked 2D layered materials for optoelectronics. 2D Materials, 2016, 3, 022001.	2.0	213
50	Serine-arginine protein kinase 1 promotes a cancer stem cell-like phenotype through activation of Wnt/β-catenin signalling in NSCLC. Journal of Pathology, 2016, 240, 184-196.	2.1	41
51	Sub-300 femtosecond soliton tunable fiber laser with all-anomalous dispersion passively mode locked by black phosphorus. Optics Express, 2016, 24, 13316.	1.7	76
52	Wavelength switchable graphene Q-switched fiber laser with cascaded fiber Bragg gratings. Optics Communications, 2016, 368, 81-85.	1.0	8
53	Broadband and enhanced nonlinear optical response of MoS2/graphene nanocomposites for ultrafast photonics applications. Scientific Reports, 2015, 5, 16372.	1.6	174
54	Few‣ayer Topological Insulator for Allâ€Optical Signal Processing Using the Nonlinear Kerr Effect. Advanced Optical Materials, 2015, 3, 1769-1778.	3.6	87

#	Article	IF	CITATIONS
55	Graphene–Bi ₂ Te ₃ Heterostructure as Saturable Absorber for Short Pulse Generation. ACS Photonics, 2015, 2, 832-841.	3.2	208
56	Microfiber-Based Highly Nonlinear Topological Insulator Photonic Device for the Formation of Versatile Multi-Soliton Patterns in a Fiber Laser. Journal of Lightwave Technology, 2015, 33, 2056-2061.	2.7	41
57	Drop-Casted Self-Assembled Topological Insulator Membrane as an Effective Saturable Absorber for Ultrafast Laser Photonics. IEEE Photonics Journal, 2015, 7, 1-11.	1.0	9
58	Generation and evolution of mode-locked noise-like square-wave pulses in a large-anomalous-dispersion Er-doped ring fiber laser. Optics Express, 2015, 23, 6418.	1.7	133
59	Wide spectral and wavelength-tunable dissipative soliton fiber laser with topological insulator nano-sheets self-assembly films sandwiched by PMMA polymer. Optics Express, 2015, 23, 7681.	1.7	108
60	Soliton fiber laser mode locked with two types of film-based Bi_2Te_3 saturable absorbers. Photonics Research, 2015, 3, A43.	3.4	73
61	Mechanically exfoliated black phosphorus as a new saturable absorber for both Q-switching and Mode-locking laser operation. Optics Express, 2015, 23, 12823.	1.7	866
62	Highly efficient tunable mid-infrared optical parametric oscillator pumped by a wavelength locked, Q-switched Er:YAG laser. Optics Express, 2015, 23, 20812.	1.7	23
63	Duration Switchable High-Energy Passively Mode-Locked Raman Fiber Laser Based on Nonlinear Polarization Evolution. IEEE Photonics Journal, 2015, 7, 1-7.	1.0	5
64	Passive Harmonic Mode-Locking in Er-Doped Fiber Laser Based on Mechanical Exfoliated Graphene Saturable Absorber. Zhongguo Jiguang/Chinese Journal of Lasers, 2015, 42, 0802013.	0.2	1
65	Visual saliency detection by DCT coefficient dissimilarity. , 2014, , .		0
66	Narrow Linewidth Q-switched Er-doped All Fiber Laser based on Topological Insulator. , 2014, , .		0
67	Large-energy, narrow-bandwidth laser pulse at 1645  nm in a diode-pumped Er:YAG solid-state laser passively Q-switched by a monolayer graphene saturable absorber. Applied Optics, 2014, 53, 254.	0.9	31
68	Stable <inline-formula> <tex-math notation="TeX">\$Q\$ </tex-math></inline-formula> -Switched Erbium-Doped Fiber Laser Based on Topological Insulator Covered Microfiber. IEEE Photonics Technology Letters, 2014, 26, 987-990.	1.3	41
69	The formation of various multi-soliton patterns and noise-like pulse in a fiber laser passively mode-locked by a topological insulator based saturable absorber. Laser Physics Letters, 2014, 11, 055101.	0.6	129
70	Nanosecond <inline-formula> <tex-math notation="TeX">\$Q\$ </tex-math></inline-formula> -Switched Erbium-Doped Fiber Laser With Wide Pulse-Repetition-Rate Range Based on Topological Insulator. IEEE Journal of Quantum Electronics, 2014, 50, 393-396.	1.0	33
71	Large Energy, Wavelength Widely Tunable, Topological Insulator Q-Switched Erbium-Doped Fiber Laser. IEEE Journal of Selected Topics in Quantum Electronics, 2014, 20, 315-322.	1.9	201
72	Electroluminescence and Photocurrent Generation from Atomically Sharp WSe ₂ /MoS ₂ Heterojunction <i>p–n</i> Diodes. Nano Letters, 2014, 14, 5590-5597.	4.5	937

#	Article	IF	CITATIONS
73	Ytterbium-doped fiber laser passively mode locked by few-layer Molybdenum Disulfide (MoS2) saturable absorber functioned with evanescent field interaction. Scientific Reports, 2014, 4, 6346.	1.6	407
74	Pulse dynamics controlled by saturable absorber in a dispersion-managed normal dispersion Tm-doped mode-locked fiber laser. Chinese Optics Letters, 2014, 12, 031405-31408.	1.3	11
75	Large-Mode-Area Double-Cladding Yb-Doped Photonic Crystal Fiber Q-Switched Mode-Locked Laser with Graphene-Based Saturable Absorber Mirror. Zhongguo Jiguang/Chinese Journal of Lasers, 2014, 41, 0402001.	0.2	0
76	Experimental study on the multisoliton pattern formation in an erbium-doped fiber laser passively mode-locked by graphene saturable absorber. Optical Engineering, 2013, 52, 044201.	0.5	7
77	Improved Transfer Quality of CVD-Grown Graphene by Ultrasonic Processing of Target Substrates: Applications for Ultra-fast Laser Photonics. ACS Applied Materials & Interfaces, 2013, 5, 10288-10293.	4.0	57
78	Multilayer graphene for Q-switched mode-locking operation in an erbium-doped fiber laser. Optics Communications, 2013, 300, 17-21.	1.0	19
79	Graphene sheet stacks for <i>Q</i> -switching operation of an erbium-doped fiber laser. Laser Physics Letters, 2013, 10, 075102.	0.6	19
80	Self-Assembled Topological Insulator: Bi\$_{2}\$Se\$_{3}\$ Membrane as a Passive Q-Switcher in an Erbium-Doped Fiber Laser. Journal of Lightwave Technology, 2013, 31, 2857-2863.	2.7	147
81	Vertically stacked multi-heterostructures of layered materials for logic transistors and complementary inverters. Nature Materials, 2013, 12, 246-252.	13.3	812
82	Wavelength-tunable picosecond soliton fiber laser with Topological Insulator: Bi_2Se_3 as a mode locker: erratum. Optics Express, 2013, 21, 444.	1.7	7
83	Third order nonlinear optical property of Bi_2Se_3. Optics Express, 2013, 21, 2072.	1.7	271
84	Large normal group velocity dispersion of micro/nano optical fiber near 2-μm wavelength. Optical Engineering, 2013, 52, 025003.	0.5	0
85	Erbium-doped fiber laser passively mode-locked by a position-adjustable graphene saturable absorber. Optical Engineering, 2012, 51, 084203.	0.5	5
86	Wavelength-tunable picosecond soliton fiber laser with Topological Insulator: Bi_2Se_3 as a mode locker. Optics Express, 2012, 20, 27888.	1.7	406
87	Ultra-short pulse generation by a topological insulator based saturable absorber. Applied Physics Letters, 2012, 101, 211106.	1.5	551
88	Switchable Dual-Wavelength Synchronously Q-Switched Erbium-Doped Fiber Laser Based on Graphene Saturable Absorber. IEEE Photonics Journal, 2012, 4, 869-876.	1.0	177
89	Microwave and optical saturable absorption in graphene. Optics Express, 2012, 20, 23201.	1.7	220
90	Passively Graphene Mode-Locked Soliton Erbium-Doped Fiber Lasers. Zhongguo Jiguang/Chinese Journal of Lasers, 2012, 39, 0602003.	0.2	1

#	Article	IF	CITATIONS
91	Wavelength-tunable passively Q-switched erbium-doped fiber laser with graphene-based saturable absorber. Qiangjiguang Yu Lizishu/High Power Laser and Particle Beams, 2012, 24, 2807-2810.	0.0	Ο
92	Core/Shell Structured Hollow Mesoporous Nanocapsules: A Potential Platform for Simultaneous Cell Imaging and Anticancer Drug Delivery. ACS Nano, 2010, 4, 6001-6013.	7.3	592